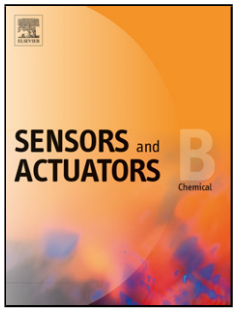

Title: The quest for highly sensitive QCM humidity sensors: the coating of CNT/MOF composite sensing films as case study

Authors: Karumbaiah. N. Chappanda, Osama Shekhah, Omar Yassine, Shashikant P. Patole, Mohamed Eddaoudi, Khaled N. Salama

PII: S0925-4005(17)32105-6
DOI: https://doi.org/10.1016/j.snb.2017.10.189
Reference: SNB 23493

To appear in: *Sensors and Actuators B*

Received date: 9-7-2017
Revised date: 14-10-2017
Accepted date: 31-10-2017

Please cite this article as: Karumbaiah.N.Chappanda, Osama Shekhah, Omar Yassine, Shashikant P.Patole, Mohamed Eddaoudi, Khaled N.Salama, The quest for highly sensitive QCM humidity sensors: the coating of CNT/MOF composite sensing films as case study, Sensors and Actuators B: Chemical https://doi.org/10.1016/j.snb.2017.10.189

The quest for highly sensitive QCM humidity sensors: the coating of CNT/MOF composite sensing films as case study

Karumbaiah. N. Chappanda[1], Osama Shekhah[2], Omar Yassine[1], Shashikant P. Patole[1], Mohamed Eddaoudi[2], Khaled N. Salama[1]

[1]Sensors Lab, Electrical Engineering Program, Computer, Electrical and Mathematical Sciences and Engineering Division, King Abdullah University of Science and Technology (KAUST), Thuwal, 23955-6900 Saudi Arabia.

E-mail: khaled.salama@kaust.edu.sa

[2]Functional Materials Design, Discovery and Development research group (FMD[3]), Advanced Membranes & Porous Materials Center (AMPMC), Physical Sciences and Engineering Division, King Abdullah University of Science and Technology (KAUST), Thuwal, 23955-6900, Saudi Arabia.

E-mail: mohamed.eddaoudi@kaust.edu.sa

ler

Highlights

- Synthesis of CNT-HKUST-1 composite thin films.
- Investigation of morphological, crystalline, and Raman-scattering characteristics of composite thin films.
- Coating of HKUST-1 and CNT-HKUST-1 thin films on QCM.
- Optimization of CNT-HKUST-1 composite ratio for enhanced humidity detection.

Abstract. The application of metal-organic frameworks (MOFs) as a sensing layer has been attracting great interest over the last decade, due to their uniform properties in terms of high porosity and tunability, which provides a large surface area and/or centers for trapping/binding a targeted analyte. Here we report the fabrication of a highly

sensitive humidity sensor that is based on composite thin films of HKUST-1 MOF and carbon nanotubes (CNT). The composite sensing films were fabricated by spin coating technique on a quartz-crystal microbalance (QCM) and a comparison of their shift in resonance frequencies to adsorbed water vapor (5 to 75% relative humidity) is presented. Through optimization of the CNT and HKUST-1 composition, we could demonstrate a 230% increase in sensitivity compared to plain HKUST-1 film. The optimized CNT-HKUST-1 composite thin films are stable, reliable, and have an average sensitivity of about 2.5 x 10^{-5} ($\Delta f/f$) per percent of relative humidity, which is up to ten times better than previously reported QCM-based humidity sensors. The approach presented here is facile and paves a promising path towards enhancing the sensitivity of MOF-based sensors.

Keywords: Metal-organic frameworks, composites, CNT, humidity, sensors.

1. Introduction

The monitoring/detection of water-vapor (humidity) using sensors is considered as one of the most frequently used application in our daily life, due to its wide uses in everyday home appliances for comfort and in industries such as the automotive, mining and manufacturing. Therefore, there is always an increasing demand for the design and development of a low-cost and highly sensitive humidity sensors [1-3] . Humidity sensors based on various transduction techniques, including acoustic [4], resistance [5, 6], magnetic [7], resonance [8], optical [9-11], impedance [12-14], delay-line [15], capacitance [16-19], and thermal [20] have been reported. Among these methods, is quartz crystal microbalance (QCM) technique, which are bulk acoustic-wave resonators, which have wide measuring range, are low-cost, small, stable, and highly sensitive to changes in mass with low detection limit, making them a preferable choice in sensing applications [21-39]. The change in mass (Δm) on the surface of the QCM is related to the shift in resonance frequency (Δf) given by the Sauerbrey equation [40]:

$$\Delta f = -\left(\frac{2 f_0^2}{A\sqrt{\rho_q \mu_q}} \right) \Delta m \qquad (1)$$

where f_0 is the fundamental resonance frequency of the QCM, ρ_q is the density of quartz crystals (2.649 gcm^{-3}), μ_q is the shear modulus (2.947×10^{10} N/m^2), and A is the area of the electrode defined on the QCM (which is sensitive to change in mass). For gas-sensing applications, QCMs alone are non-functional, as they require an additional layer (i.e. sensing layer) that induces a change in mass and/or viscoelastic characteristics on the surface when exposed to the target gas [21-39]. QCMs for humidity sensing application have been intensively studied by coating them with different water-adsorbing materials, such as polymers [21, 23, 25, 26, 30, 31, 33, 34, 36, 39], oxides [21, 23, 25, 28, 32, 34, 36, 37], nano-structures [21-23, 25, 27-30, 32, 33, 35-39], and composites [21, 23, 25, 26, 29, 30, 36, 39]. Among them is the new class of crystalline porous materials called metal-organic frameworks (MOFs), which have recently gained more interest for various sensing applications [18, 24]. MOFs are crystalline and highly porous materials that are made of interlinked organic and non-organic building units [41-44]. The reversible sorption behavior of MOFs, their structure and chemical tunability put forward their potential for gas-sensing purposes. The coating of MOFs on the QCM electrodes allows to measure the change of the mass of the materials, which is caused by adsorption or desorption of molecules by the MOF layer, which could be utilized to detect small amounts of targeted gaseous analytes [45]. MOFs have been used to detect various gases/vapors such as H_2O, O_2, H_2S, and many volatile organic compounds (VOCs) [18, 24, 46-48]. HKUST-1 is one of the MOFs, which is highly porous and consists of Cu(II) paddle wheel building unit interconnected by 1, 3, 5- Benzene tricarboxylic acid linkers, which provide a three dimensional structure with large surface area and open metal sites [49]. HKUST-1 is especially promising for detecting water vapor compared to organics and polymer films, as it can absorb water up to 40 wt% [50]. Previous reports describe the use of micro-beams and QCMs coated with HKUST-1 to detect humidity and other vapors [24, 50, 51]. However, very little work has been directed towards increasing the sensitivity of HKUST-1 thin films. One of the methods to increase the sensitivity of MOFs like HKUST-1, is to mix it with another type of material to form a composite that combine the advantages of the different properties of the two starting materials. In principle, there are two types of composite materials, which can be fabricated using the following approaches. In the first approach, nano-sized

structures/particles are used as the skeletal and is added, in order to enhance the surface area of the primary humidity sensitive material [21, 30, 34, 36, 39]. In the second approach, two or more humidity sensitive materials are mixed/combined to form composites, which will lead to the enhancement of the overall sensitivity [23, 25, 26]. In this work, we combine the advantages of the two approaches, where both the materials used (HKUST-1 and CNT) are individually nano-structured/porous (which possess/provide enhanced surface area) [18, 24, 29, 35, 38]. In addition to that, they are both sensitive to change in humidity [18, 24, 29, 35, 38], which will complement each other and potentially lead to improving the overall sensitivity of the composite. This improved sensitivity could yield enhanced device performance, in comparison to the two types of traditional composites.

In this study, we synthesize composite materials consisting of CNT and HKUST-1 MOF, in which, both the CNT and the HKUST-1 MOF are individually/independently porous and are sensitive to humidity [24, 29, 35, 38]. Using the optimized CNT-HKUST-1 composite thin films, we report a simple method for sensor development with enhanced sensitivity. These composite films can act as a selective sensing layer that can be easily deposited onto QCM electrodes. The use of this CNT-HKUST-1 MOF composite make their integration facile and compatible with existing fabrication techniques, which will allow to measure and compare the response of blank QCM, QCM coated with CNT, HKUST-1 and CNT-HKUST-1 composite (of different ratios) thin films, to the change in relative humidity. In this study, we report the short and long-term stability of the sensor in addition to its sensitivity dependence on temperature variation.

2. Material and methods

2.1 Material preparation and experimental setup

The base solution of HKUST-1 was synthesized in accord with previously reported method [52-55]. Different composites were prepared by dispersing different weight of 0.2, 0.5, 1.5, and 2.5 mg of multi-walled carbon nanotubes (MWCNT) from Sigma Aldrich (cat. No. 659258), respectively in 2.5 g of

HKUST-1 base solution by ultra-sonicating for 1 hr. The nanotubes were 100 to 200 nm in diameter and 5 to 11 μm in length [56]. In addition to that, 1 mg of CNT was dispersed in 2.5 g of isopropanol to form the plain CNT mixtures, which we use as a reference. The base mixtures were spin-coated at 1000 RPM for 120 s on 5.932 MHz AT-cut QCMs with 5 mm diameter Au electrodes (Fig 1 (a)). The coated QCMs were then cured on a hot plate at 50 ^{o}C for 1 h to evaporate the solvents and form the MOF and CNT-MOF composite thin films. The thickness of the deposited HKUST-1 and CNT-HKUST-1 films on the QCM were found to be typically between 2 to 3 μm (Fig 1 (b)). The CNT- isopropanol mixture was drop-casted on the QCM and air dried multiple times until a uniform visible layer was formed. The QCMs were then exposed to humidity in a LabVIEW automated measurement setup (Fig. 2) [18, 57-60]. The setup consists of two micro-flow controllers (MFCs) from Alicat Scientific Inc. and a computer with LabVIEW to control/monitor the gas flow. A thermostatic bath (Chiller F12-MA by Julabo) (also controlled by computer) with a glass bubbler was used as humidifier. An airtight custom built test chamber (volume of 400 cm^3) with a XAVAC 15M hermetic feedthrough connector from Positronic (used for probing the commercial and QCM sensors) was used for characterizing the device. A hot plate (Torrey Pines Scientific EcoTherm HS60) was placed underneath to heat the chamber. D.C. power supplies and voltmeters were used for biasing/monitoring the commercial humidity and temperature sensors (data acquired by computer). The maximum flow of the MFCs was limited to 200 cm^3/min. One of the MFC was used for passing dry N_2 or air into the chamber. The other MFC was used for controlling the flow of air/N_2-water mixture (generated by bubbling in water) into the test chamber. Stainless steel pipes with valves (from Swagelok) or perfluoroalkoxy alkane tubing (in regions requiring flexibility) were used as delivery lines. The temperature of the thermostatic bath was maintained at 17 ± 0.03 ^{o}C at all time. The temperature inside the chamber was at 20 ± 0.5 ^{o}C at all time unless specified. The setup was tested for leakage using a vacuum pump. The change in resonance frequency was monitored using a two-port network analyzer (Keysight E5071C ENA) circuit. Alternating frequency sweeps in the forward direction at 70.7 V_{RMS} were used to measure the S_{21} parameters of the QCM resonator. An HIH-4000-003 commercial humidity sensor from Honeywell was used as a reference which has an error less than 0.5 %RH. LM35DZ/NOPB commercial temperature sensor from Texas

Instruments was used to monitor the temperature inside the test chamber which has an error less than 0.5 ^{o}C. Please note that there are additional components shown in Fig. 2 (b) and was not used in characterizing the sensors.

2.2 Material characterization

The same set of base mixtures were also coated and cured on 2 x 2 cm Si dies for scanning electron microscope (SEM), Raman spectroscopy, and X-ray diffraction (XRD) analysis. The MOF and CNT-MOF composites were sputter coated with a 3 nm iridium layer to reduce charging during SEM morphological analysis. Raman analysis was performed in a Horiba Aramis Spectrometer using a 473 nm laser source at a power below 10 mW with a 50X objective lens. The base mixtures were drop cast on holey carbon Cu grid for analysis by transmission electron microscopy (TEM) in FEI Tecnai G^2 80-300 ST (imaged at 300 kV). Electron micrographs were recorded on a 4 x 4 k pixel-charged couple device (CCD) camera (Gata, Inc., US4000). The XRD characterization was performed on a PANalytical X'Pert PRO MPD X-ray diffractometer at 45 kV, 40 mA for CuKα (λ = 1.5418 Å).

3. Results and discussions

3.1 Characteristics of the composite films

In this study, in addition to plain HKUST-1 and CNT thin films, CNT-HKUST-1 composites of different weight ratios were prepared by dispersing different weight ratios of CNT with HKUST-1 base solution by ultra-sonication technique. The base mixtures were spin-coated on QCMs and cured on a hot plate at 50 ^{o}C for 1 h to evaporate the solvents and form the MOF and CNT-MOF composite thin films. The false-color SEM micrographs of HKUST-1 and CNT-HKUST-1 composite are shown in Fig. 3. The SEM images (Fig. 1 (b)) shows the formation of an HKUST-1 thin film composed of crystals with cubical morphology, which are akin to crystals synthesized at low temperatures [61]. Uniform dispersion of CNT in the HKUST-1 crystal-thin films is achieved by ultra-sonication and spin coating of the CNT-HKUST-1 precursor composite. Noticeably, we found that the average crystal size of HKUST-1 MOF is

significantly affected due to the presence of CNT in the composite films. It is to be noted that small clusters of bundled CNT were present in the composite thin films due to coagulation during the curing process. Fig. 3 (a) shows the SEM micrograph of a composite thin film with a low concentration of CNT (lower than 0.2 mg). At very low concentrations, the thin films formed at the regions surrounding the random CNT exhibit reduced crystal size compared to the regions without the CNT. Figs. 3 (b)-(d) shows the SEM micrographs of CNT-HKUST-1 composites with 0.5, 1.5 and 2.5 mg CNT, respectively. The decrease in the HKUST-1 crystal size in the presence of dispersed CNT may be due to the reason as follows. As the base solution is cured, random seed crystals are formed at the nucleation sites on the surface of the substrate upon which the MOF crystals continue to grow. The presence of CNT increases the number of nucleation sites [62], subsequently increasing the effective surface area for the growth of HKUST-1 crystals. This leads to reduction in the average crystal size and increases the number of MOF crystals formed. At higher concentration and near-uniform dispersion of CNT, the crystal size was reduced throughout the thin film. The presence of MOF crystal-growth nucleation sites on the surface of the CNT was corroborated by TEM and high-resolution TEM images (Fig. 4). Fig. 4(a) shows that cubical HKUST-1 crystals are formed on the surface of the CNT. In addition to that, the average size of the crystals formed are smaller than that of plain HKUST-1 crystals (in comparison to Fig. 1(a)). Fig. 4(b) shows a HRTEM image of HKUST-1 crystals, which are formed/adhered on the surface of the CNT. Raman spectra of the CNT, HKUST-1, and CNT-HKUST-1 composite thin films are shown in Fig. 5. Raman peaks around 1370, 1580, and 2740 cm^{-1} correspond to the D, G, and 2D bands of MWCNT [63]. Low D/G ratios detect highly crystalline and graphitic MWCNT. No Raman peaks corresponding to CNT were detected in the plain HKUST-1 thin film. With the increase in the CNT ratios of the CNT-HKUST-1 composites, the intensity of the CNT Raman peaks also increased, thereby corroborating the dispersion process. Low Raman-scattering peaks at 177, 275, 448, and 502 cm^{-1} were contributed by the Cu(II) ions of the HKUST-1 crystals [64]. Raman peaks at 740, 826, and 2923 cm^{-1} are associated to the C-H bonds. Raman peaks at 1006 and 1610 cm^{-1} are due to the presence of the C=C bond of the benzene ring. Raman peaks at 1460 and 1550 cm^{-1} are contributed by symmetric and asymmetric COO-carboxylate units. There

was no noticeable change/shift in the corresponding HKUST-1 Raman peaks in the composite thin films, confirming the integrity of the HKUST-1 chemical characteristics. Fig. 6 shows the comparison of the XRD pattern of bulk HKUST-1 with CNT-HKUST-1 composite thin film. The CNT-HKUST-1 composite thin film is in excellent agreement with the calculated bulk HKUST-1 spectrum, supporting the formation of the HKUST-1 MOF crystal structure even in the presence of CNT.

3.2 Characteristics of the humidity sensor

Fig. 7 shows a comparison of the S_{21} frequency spectrum, at various relative-humidity points, of QCM sensors coated with CNT, HKUST-1, and CNT-HKUST-1 composite thin films. The QCM response has two regions that consist of resonance and anti-resonance peaks. The anti-resonance peaks are due to device-parasitic currents. However, the resonance peaks are used as the reference for monitoring the effect of adsorbed mass as a result of the change in humidity. With the increase in humidity, the resonant peaks of sensors decrease in frequency and experience gradual damping. Also, the bandwidth of the resonant peaks broadens, induced by damping, due to the increase in mass uptake by the sensing layer. 0.5 mg CNT-HKUST-1 composite thin films experience the maximum shift in frequency and resonant bandwidth damping with change in humidity. Fig. 8 shows a comparison of the shift in resonance frequency ($\Delta f/f$) caused by a change in relative humidity (RH) from 5 to 75% of the QCM with uncoated, CNT, plain HKUST-1, and CNT-HKUST-1 composite thin films. Δf is the shift in QCM resonance frequency due to adsorbed water vapor, and f is the resonance frequency of the QCM. Uncoated QCM show a negligible shift in resonance frequency due to change in humidity. QCM coated with CNT exhibit a low response to humidity. From 5 to 15% RH, the CNT coated QCM exhibited a higher sensitivity of -27.8 Hz per percent RH. From 15 to 75% RH, the sensitivity of the device was reduced to -6.5. Hz per percent RH. Overall, the CNT thin film demonstrates lower sensitivity than previously reported CNT-coated QCM humidity sensors [29, 35, 38]. This may be due to the difference in the amount, structural morphology, and synthesis technique of the CNT thin films. Plain HKUST-1 thin films produce non-linear frequency shifts in response to change in humidity, with an average sensitivity

of -61.5 Hz per percent RH. The sensitivity varied between -32 to -84 Hz per percent RH between the range 5 to 75% RH. The sensitivity of the CNT-HKUST-1 composite thin films to humidity were higher, among which, the 0.5 mg composite film demonstrates the highest sensitivity. The average sensitivity of the 0.5 mg composite film is -141 Hz per percent RH ($\{\Delta f/f\}$ per percent RH = -2.5 x 10^{-5}), which is 230% higher than plain HKUST-1 film. The sensitivity due to non-linearity varied between -92 to -280 Hz per percent RH. The average sensitivity of the 1.5 and 2.5 mg CNT-HKUST-1 composite thin films is about -119 and -97 Hz per percent RH, respectively. The difference in the average sensitivity of the humidity-sensing films may be due to the difference in the overall crystal size of the deposited films which affects the water sorption kinetics. Uehara et al. demonstrated that the gas sorption kinetics of the HKUST-1 films can be enhanced by downsizing the film's crystal size [65]. Also, with reduced crystal size, the surface area may be affected/increased, leading to increase in film sensitivity. In the plain HKUST-1 thin film, the average crystal size is higher, resulting in lower sorption and sensitivity to humidity. However, in the composite thin films, the average crystals size is reduced due to the presence of CNT, thereby increasing the water vapor sorption kinetics and sensitivity of the films. However, the highest sensitivity seen in 0.5 mg CNT composite thin films may be due to the presence of an optimized number of CNT which provides optimized nucleation sites, crystal size and surface area. Though, higher CNT concentration downsizes the crystals, the overall sensitivity of the sensor will be reduced due to the lower affinity of CNT towards water. On the other hand, lower concentration of CNT does not sufficiently downsize the crystals and in turn do not sufficiently enhance the sensitivity. In other words, the concentration of the CNT in the composite thin films is to be optimized such that the size of HKUST-1 crystals is reduced without reducing the overall sensitivity due to the presence of excess CNT in the thin films.

Another factor that affects the sensitivity of the film is the mass of the humidity sensitive films [32, 35]. Table 1 compares the mass of the coated sensing films and their corresponding adsorbed water wt% at 75% humidity (estimated using Sauerbrey equation [40]). By addition of CNT to the HKUST-1 base solution, it can be seen that the mass of the spin coated humidity sensitive film increases. This may be due

to the increase in the viscosity of the composite base solution (higher viscosity yields thicker spin coated film) as well as due to the additional mass of the CNT. The composite films have up to 78% higher mass in comparison to the plain HKUST-1 films and hence have higher sensitivity to change in humidity. However, by comparing the absorbed water wt% at 75% RH, it can be seen that the 0.5 mg CNT-HKUST-1 films have 33% higher absorbed water wt% when compared to the plain HKUST-1 film. With further increase in the CNT ratio, the absorbed water wt% decreases. In case of 2.5 mg CNT-HKUST-1 films, it can be seen that absorbed water wt% is almost equal to that of plain HKUST-1 films. This corroborates that the presence of optimized CNT ratio in the composite films increases the overall sensitivity due to increase in film mass as well as increased surface area. Plain CNT film has the lowest absorbed water wt% of about 10.

3.3 Hysteresis, stability, response/recovery time and effect of temperature

An important parameter to evaluate the performance of humidity sensors is the hysteresis curve, which is defined by the maximum difference during the adsorption and desorption cycle of the sensor [13-15]. This characteristic was examined by exposing the sensor to increasing (from 5 to 75%) and decreasing (from 75 to 5%) RH environment. Fig. 9 shows the hysteresis of humidity sensor coated with 0.5 mg CNT-HKUST-1 composite thin films. The reverse/desorption cycle lags from the forward/adsorption cycle by a maximum of about less than 5% RH at around 40% RH, demonstrating low hysteresis and indicating that the humidity sensor showed good reliability. The low hysteresis exhibited by the sensor characteristics may be due to the difference in the chemical nature of HKUST-1 during the adsorption and desorption process. Further, the short-term and the long-term stability of the sensor were studied. In the short-term stability study, the sensor was exposed to constant humidity for 60 mins, and the output frequency response was monitored at a time interval of 4 mins (Fig. 10 (a)). The output frequency fluctuation was less than 50 Hz, demonstrating stable short-term stability of the sensor, which is suited for high precision humidity sensors. The long-term stability of the sensor was analyzed by measuring the sensor response after every 24 hours, over a period of 10 days (Fig. 10 (b)). Overall, the

sensor presented here, demonstrated good long and short-term stability, as required in highly sensitive and stable humidity sensors. Further, the response and recovery time of the sensor is characterized. The chamber was initially set at 5% RH and then increased to 75% RH for measuring the response time. Similarly, the chamber was purged with dry N_2 to revert the humidity in the chamber to 5% RH. Fig. 11 shows the response and recovery characteristics of the sensor. The response and recovery time of is defined as the time required to reach 90% of the total frequency response. The response time and recovery time was less than 4.2 and 4.4 mins, respectively. Our current setup is limited in terms of measuring the actual response and recovery time of the sensor due to the maximum flow rate limitation of the MFCs (200 cm^3/min). This requires longer time for the humidification and dehumidification of the chamber. For comparison, Fig. 11 (red line) also shows the response and recovery of the commercial humidity sensor, and the QCM humidity sensors is in par with the commercial humidity sensor.

Another important factor to be analyzed is the effect of temperature on the sensor performance. The temperature of the chamber was heated using a hot plate. This increases the temperature of the chamber and the sensor. The commercial temperature sensor and the device under test was placed at the same vertical distance from the hot plate inside the chamber to minimize the error due to the presence of temperature gradient inside the test chamber. The test chamber was purged with dry N_2 overnight at room temperature to eliminate the presence of any water vapor. Fig. 12 (a) shows the effect of temperature on the commercial sensor at near zero %RH. The sensors showed negligible drift in voltage output (corresponding %RH values at 20 ^oC are shown in Fig. 12 (a)), making them suitable for high temperature studies. Further, the effect of temperature on QCM coated with 0.5 mg CNT-HKUST-1 composite thin film was analyzed (Fig. 12 (b)). The temperature of the bubbler was set at 17 ^oC. The flow of the dry N_2 and the N_2 + water was set such that the RH is fixed at 55 % at 20 ^oC. With increase in temperature, the sensor experienced an increase in resonant frequency with a sensitivity of 0.056 x $10^{-4}/^oC$ ($\Delta f/f_t$, where f_t is the frequency of the QCM coated sensor at room temperature, 20 ^oC). This positive sensitivity response of the sensor is due to the reduced humidity sorption capability of the HKUST-1 crystals at elevated temperatures. However, the effect of temperature is relatively insignificant compared to the sensitivity of

the device due to change in humidity, making the sensor operational at elevated temperatures of up to 60 ^{o}C. Note that, with increase in the temperature, the RH values at the elevated temperature is different from initial RH at room temperature [66]. However, the presence of water vapor content remains the same due to the fixed dry N_2 and the N_2 + water flow. The corresponding %RH at elevated temperature is shown in Fig. 12 (b).

3.4 Sensor response due to change in relative humidity in air

An important requirement for practical implementation of the humidity sensor is to study the response in air. The base gas was changed from N_2 to air and the response of the sensor due to change in humidity was characterized. The air gas consisted of 79.5% N_2 and 20.5% O_2 by volume. Fig. 13 shows the QCM coated with 0.5 mg CNT-HKUST-1 sensor response to change in humidity with air as the base gas. The average sensitivity is -134 Hz per percent RH ($\{\Delta f/f\}$ per percent RH = -2.3×10^{-5}). The same sensor when characterized in N_2 as the base gas showed negligible difference in response with change in relative humidity (red line). This shows that presence of 20.5% oxygen in the base gas did not affect the device performance. Further, the sensor was also characterized in 400 ppm of CO_2 (commonly present in air) and has no noticeable response. This shows that the sensor is promising for practical application in air as a humidity sensor.

Table 2 shows the comparison of the material coated, range of relative humidity, and sensitivity of the previously published work on QCM based humidity sensors. The technique used for synthesizing the humidity sensitive composite films is simple and relatively easy. It does not involve the use any high voltage sources (20 kV), as required for synthesizing polyacrylic acid [33] and polyethyleneimine [30] humidity sensitive membranes. The use of harsh/corrosive chemicals such as HCL [26, 34], KOH [28], H_2SO_4 [29], and HNO_3 [29, 35, 38] are avoided, making our synthesis technique, a relatively environmental friendly process. The dispersion process is relatively faster and does not require long ultra-sonication [22], stirring [34] or milling process [38]. The composite films here are synthesized at 50 ^{o}C, making it a low cost process compared to previous reports, which require high temperatures above 500 ^{o}C [27, 34, 37, 38]. Lastly, the sensitivity demonstrated by 0.5 mg CNT-HKUST-1 composite thin film is up

to ten times better when compared to the previously reported QCM-based humidity sensors, thereby making it a promising approach towards, simple, low-cost, low-power, stable, reliable and highly sensitive humidity sensors.

4. Conclusions

Here we report the fabrication of CNT-HKUST-1 composite thin films on QCM electrode and applied them for humidity detection. In this work, we have compared the performances of blank QCM, QCM coated with CNT, HKUST-1 and CNT-HKUST-1 composite thin films for detecting humidity. HKUST-1 thin film with 0.5 mg CNT demonstrated the highest humidity sensitivity of -141 Hz per percent RH, which is about 230% higher than that of plain HKUST-1 thin film. The reported $\Delta f/f$ of the device is on par with or better than most previously demonstrated humidity sensors with low hysteresis and stable response, thereby making it a promising candidate for practical and highly sensitive humidity detection. The sensitivity-enhancement methodology presented here is simple and could be used to increase the sensitivity of other MOF-based gas sensors.

Competing interests

The authors declare that they have no competing interests.

Acknowledgment

This work was partially sponsored by the Advanced Membranes and Porous Materials Center (AMPMC)'s grant FCC/1/1972-05-01 within the "Stimuli Responsive Materials" thrust. We thank Ulrich Buttner of 'Microfluidic Lab, part of the Nanofabrication Core Lab', for providing his assistance in the project.

References

[1] N. Yamazoe, Y. Shimizu, Humidity sensors: principles and applications, Sens. Actuators 10 (1986) 379–398.
[2] A.E. Dessler, S.C. Sherwood, A matter of humidity, Science 323 (2009) 1020–1021.
[3] T.A. Blanka, L.P. Eksperiandova, K.N. Belikova, Recent trends of ceramic humidity sensors development: A review, Sens. Actuators B 228 (2016) 416–442.
[4] M. Penza, G, Cassano, Relative humidity sensing by PVA-coated dual resonator SAW oscillator, Sens. Actuators B 68 (2000) 300–306.
[5] K.-J. Park, M.-S. Gong, A water durable resistive humidity sensor based on rigid sulfonated polybenzimidazole and their properties, Sens. Actuators B 246 (2017) 53–60.
[6] A. Quddious, S. Yang, M.M. Khan, F.A. Tahir, A. Shamim, K. N. Salama, H.M. Cheema, Disposable, Paper-Based, Inkjet-Printed Humidity and H_2S Gas Sensor for Passive Sensing Applications, Sensors 16 (2016) 2073.
[7] D. Matatagui O.V. Kolokoltsev, N. Qureshi, E.V. Mejía-Uriarte, J.M. Saniger, A novel ultra-high frequency humidity sensor based on a magnetostatic spin wave oscillator, Sens. Actuators B 210 (2015) 297–301.
[8] R.G. Hennessy, M.M. Shulaker, M. Messana, A.B. Graham, N. Klejwa, J. Provine, T.W. Kenny, R.T. Howe, Vacuum encapsulated resonators for humidity measurement, Sens. Actuators B 185 (2013) 575–581.
[9] L. Xu, J.C. Fanguy, K. Soni, S. Tao, Optical fiber humidity sensor based on evanescent-wave scattering, Opt. Lett. 29, (2004) 1191–1193.
[10] Chowdhury, F.K., K.N. Chappanda, and M. Tabib-Azar. *High enhancement SERS substrates created using DEP-DLA & annealing Au-W*. in *Sensors, 2011 IEEE*. 2011. IEEE.
[11] W. Yuan, K. N. Chappanda, M. Tabib-Azar, Microfabricated atmospheric RF microplasma devices for gas spectroscopy, in 15th International Conference on Miniaturized Systems for Chemistry and Life Sciences, MicroTAS (2011), 568-570.
[12] Z. Zhuang, Y. Li, D. Qi, C. Zhao, H. Na, Novel polymeric humidity sensors based on sulfonated poly (ether ether ketone)s: Influence of sulfonation degree on sensing properties, Sens. Actuators B 242 (2017) 801–809.
[13] J. Dai, T. Zhanga, H. Zhao, Teng Fei, Preparation of organic-inorganic hybrid polymers and their humidity sensing properties, Sens. Actuators B 242 (2017) 1108–1114.
[14] S. Samai, C. Sapsanis, S.P. Patil, A. Ezzeddine, B.A. Moosa, H. Omran, A.-H. Emwas, K.N. Salama, N.M. Khashab, Light Responsive Two-Component Supramolecular Hydrogel: A Sensitive Platform for Humidity Sensors, Soft Matter 12 (2016) 2842-2845.
[15] H.-S. Hong, D,-T. Phan, G.-S. Chung, High-sensitivity humidity sensors with ZnO nanorods based two-port surface acoustic wave delay line, Sens. Actuators B 171–172 (2012) 1283–1287.
[16] E. Esmaeli, M. Ganjiana, H. Rastegar, M. Kolahdouz, Z. Kolahdouz, G. Q. Zhang, Humidity sensor based on the ionic polymer metal composite, Sens. Actuators B 247 (2017) 498–504.
[17] M. Sajid, H. B. Kim, Y. J. Yang, J. Jo, K. H. Choi, Highly sensitive BEHP-co-MEH:PPV + Poly(acrylic acid) partial sodium salt based relative humidity sensor, Sens. Actuators B 246 (2017) 809–818.
[18] C. Sapsanis, H. Omran, V. Chernikova, O. Shekhah, Y. Belmabkhout, U. Buttner, M. Eddaoudi, K.N. Salama, Insights on Capacitive Interdigitated Electrodes Coated with MOF Thin Films: Humidity and VOCs Sensing as a Case Study, Sensors 15 (2015) 18153 –18166.
[19] K. N. Chappanda, M. Tabib-Azar, Electrical and AFM Structural Studies of a Humidity Sensors Based on Keratin (Human Hair), In IEEE Sensors (2011), 1062-1065.
[20] M. Kimura, A new method to measure absolute humidity independently of the ambient temperature, Sens. Actuators B 33 (1996) 156–160.

[21] R. Lv, J. Peng, S. Chen, Y. Hu, M. Wang, J. Lin, X. Zhou, X. Zheng, A highly linear humidity sensor based on quartz crystal microbalance coated with urea formaldehyde resin / nano silica composite films, Sens. Actuators B 250 (2017), 721-725.
[22] Y. Yao, H. Zhang, J. Sun, W. Ma, L. Li, W. Li, J. Du, Novel QCM humidity sensors using stacked black phosphorus nanosheets as sensing film, Sens. Actuators B 244 (2017) 259–264.
[23] Z. Yuan, H. Tai, Z. Ye, C. Liu, G. Xie, X. Du, Y. Jiang, Novel highly sensitive QCM humidity sensor with low hysteresis based on graphene oxide (GO)/poly(ethyleneimine) layered film, Sens. Actuators B 234 (2016) 145–154.
[24] L. Kosuru A. Bouchaala, N. Jaber, M.I. Younis, Humidity Detection Using Metal Organic Framework Coated on QCM, J. Sensors 2016 (2016), 4902790.
[25] X. Chen, X. Chen, N. Li, X. Ding, X. Zhao, A QCM Humidity Sensors Based on GO/Nafion Composite Films With Enhanced Sensitivity, IEEE sensors 16 (2016) 8874–8883.
[26] S. D. Zor, H. Cankurtaran, QCM Humidity Sensors Based on Organic/Inorganic Nanocomposites of Water Soluble-Conductive Poly(diphenylamine sulfonic acid), Int. J. Electrochem. Sci. 11 (2016) 7976 – 7989.
[27] Y. Yao, X Chen, W. Ma, W. Ling, Quartz Crystal Microbalance Humidity Sensors Based on Nanodiamond Sensing Films, IEEE trans. Nanotech. 13 (2014) 386–393.
[28] N. Sakly, A.H. Said, H.B. Ouada, Humidity-sensing properties of ZnO QDs coated QCM: Optimization, modeling and kinetic investigations, Mater Sci Semicond Process. 27 (2014) 130–139.
[29] H. Jing, Y. Jiang, X. Du, H. Tai, G. Xie, Humidity sensing properties of different single-walled carbon nanotube composite films fabricated by layer-by-layer self-assembly technique, Appl Phys A 109 (2012) 111–118.
[30] X. Wang, B. Ding, J. Yu, M. Wang, Highly sensitive humidity sensors based on electro-spinning/netting a polyamide 6 nano-fiber/net modified by polyethyleneimine, J. Mater. Chem. 21 (2011) 16231–16238.
[31] W. Hu, S Chen, B. Zhou, L Liu, B Ding, H Wang, Highly stable and sensitive humidity sensors based on quartz crystal microbalance coated with bacterial cellulose membrane, Sens. Actuators B 159 (2011) 301–306.
[32] Y. Yao, X. Chen, H. Guo, Z. Wu, Graphene oxide thin film coated quartz crystal microbalance for humidity detection, Appl. Surf. Sci. 257 (2011) 7778–7782.
[33] X. Wang, B. Ding, J. Yu, M. Wang, F. Pan, A highly sensitive humidity sensor based on a nanofibrous membrane coated quartz crystal microbalance, Nanotechnology 21 (2010) 055502.
[34] Y. Zhu, H. Yuan, J. Xua, P. Xuc, Q. Pan, Highly stable and sensitive humidity sensors based on quartz crystal microbalance coated with hexagonal lamelliform monodisperse mesoporous silica SBA-15 thin film, Sens. Actuators B 144 (2010) 164–169.
[35] K. Jaruwongrungsee A. Wisitsoraat, A. Tuantranont, T. Lomas, Humidity sensor utilizing multiwalled carbon nanotubes coated quartz crystal microbalance, In Nanoelectronics Conference, 2008. INEC 2008. 2nd IEEE International (2008) 961–964.
[36] P.G. Su, Y.-P. Chang, Low-humidity sensor based on a quartz-crystal microbalance coated with polypyrrole/Ag/TiO_2 nanoparticles composite thin films, Sens. Actuators B 129 (2008) 915–920.
[37] X. Zhou, J. Zhang, T. Jiang, X. Wang, Z. Zhu, Humidity detection by nanostructured ZnO: A wireless quartz crystal microbalance investigation, Sens. Actuators A 135 (2007) 209–214.
[38] Y. Zhang K. Yu, R. Xu, D. Jiang, L. Luo, Z. Zhu, Quartz crystal microbalance coated with carbon nanotube films used as humidity sensor, Sens. Actuators A 120 (2005) 142–146.
[39] H.-W. Chen, R.-J. Wu, K.-H. Chan, Y.-L. Sun, P.-G. Su, The application of CNT/Nafion composite material to low humidity sensing measurement, Sens. Actuators B 104 (2005) 80–84.
[40] G. Sauerbrey, The use of quartz oscillators for weighing thin layers and for microweighing applications, Z. Phys. 155 (1959) 206–222.
[41] O. Shekhah, L. Fu, R. Sougrat, Y. Belmabkhout, A.J. Cairns, E.P. Giannelis, M. Eddaoudi, Successful implementation of the stepwise layer-by-layer growth of MOF thin films on confined surfaces: mesoporous silica foam as a first case study, Chem. Commun. 48 (2012) 11434−11436.

[42] O. Shekhah, M. Eddaoudi, The liquid phase epitaxy method for the construction of oriented ZIF-8 thin films with controlled growth on functionalized surfaces, Chem. Commun. 49 (2013) 10079-10081.
[43] H. Streit, M. Adlung, O. Shekhah, X. Stammer, H.K. Arslan, O. Zybaylo, T. Ladnorg, H. Gliemann, M. Franzreb, C. Wöll, C. Wickleder, Surface-Anchored MOF-Based Photonic Antennae, Chem. Phys. Chem., 3 (2012) 2699−2702.
[44] O. Shekhah, C. Busse, A. Bashir, F. Turcu, X. Yin, P. Cyganik, A. Birkner, W. Schuhmann, C. Wöll, Electrochemically deposited Pd islands on an organic surface: the presence of Coulomb blockade in STM I(V) curves at room temperature, Phys. Chem. Chem. Phys. 29 (2006) 3375−3378.
[45] O. Shekhah, H.K. Arslan, K. Chen, M. Schmittel, R. Maul, W. Wenzel, C. Wöll, Post-synthetic modification of epitaxially grown, highly oriented functionalized MOF thin films, Chem. Commun. 47 (2011), 11210-11212.
[46] R. Xu, Y. Wang, X. Duan, K. Lu, D. Micheroni, A. Hu, W. Lin, Nanoscale Metal–Organic Frameworks for Ratiometric Oxygen Sensing in Live Cells, J. Am. Chem. Soc. 138 (2016) 2158–2161.
[47] O. Yassine, O. Shekhah , A.H. Assen, Y. Belmabkhout, K.N. Salama, M. Eddaoudi, H_2S Sensors: Fumarate-Based fcu-MOF Thin Film Grown on a Capacitive Interdigitated Electrode, Angew. Chem. Int. Ed. 55 (2016) 15879–15883.
[48] H. Yamagiwa, S. Sato, T. Fukawa, T. Ikehara, R. Maeda, T. Mihara, M. Kimura, Detection of Volatile Organic Compounds by Weight-Detectable Sensors coated with Metal-Organic Frameworks, Sci. Rep. 4 (2014) 6247.
[49] O. Shekhah, J. Liu, R.A. Fischer, Ch. Wöll, MOF thin films: existing and future applications. Chem. Soc. Rev. 40 (2011) 1081-1106.
[50] M.D. Allendorf, R.J.T. Houk, L. Andruszkiewicz, A.A. Talin, J. Pikarsky, A. Choudhury, K. A. Gall, P. J. Hesketh, Stress-induced chemical detection using flexible metal-organic frameworks," J. Am. Chem. Soc. 130 (2008) 14404–14405.
[51] I. Ellern, A. Venkatasubramanian, J.H. Lee, P.J. Hesketh, V. Stavila, M.D. Allendorf, A.L. Robinson, Characterization of piezoresistive microcantilever sensors with metal organic frameworks for the detection of volatile organic compounds, ECS Trans. 50 (2013) pp. 469–476.
[52] O. Shekhah, N. Roques, V. Mugnaini, C. Munuera, C. Ocal, J. Veciana, C. Wöll, Grafting of Monocarboxylic Substituted Polychlorotriphenylmethyl Radicals onto a COOH-Functionalized Self-Assembled Monolayer through Copper (II) Metal Ions, Langmuir 27 (2011) 12261.
[53] E.M.S. Azzam, A. Bashir, O. Shekhah, A.R.E. Alawady, A. Birkner, Ch. Grunwald, Ch. Wöll., Fabrication of a surface plasmon resonance biosensor based on gold nanoparticles chemisorbed onto a 1, 10-decanedithiol self-assembled monolayer, Thin Solid Films 518 (2009) 387-391.
[54] P. St Petkow, G.N. Vayssilov, J. Liu, O. Shekhah, Y. Wang, C. Wöll, T. Heine, Defects in MOFs: A Thorough Characterization, ChemPhysChem 13 (2012) 2025-2029.
[55] J. L. Zhuang, D. Ar, X. J. Yu, X. J Liu, A. Terfort, Patterned Deposition of Metal-Organic Frameworks onto Plastic, Paper, and Textile Substrates by Inkjet Printing of a Precursor Solution, Adv. Mater. 25 (2013) 4631–4635.
[56] K.N. Chappanda, N.M. Batra, J. Holguin, P.M.F.J. Costa, M.I. Younis, Fabrication and Characterization of MWCNT-Based Bridge Devices, IEEE Trans. Nanotechnol. (2017) DOI: 10.1109/TNANO.2017.2742149.
[57] H. Omran, M. Arsalan, K. N. Salama, An Integrated Energy-Efficient Capacitive Sensor Digital Interface Circuit, Sens. Actuators A 216 (2014) 43–51.
[58] A. Alhoshany, H. Omran, K. N. Salama, A 45.8fJ/Step, Energy-Efficient, Differential SAR Capacitance-to-Digital Converter for Capacitive Pressure Sensing, Sens. Actuators A 245 (2016) 10–18.
[59] H. Omran, A. Alhoshany, H. Alahmadi, K. N. Salama, A 33fJ/Step SAR Capacitance-to-Digital Converter Using a Chain of Inverter-Based Amplifiers, IEEE Trans. Circuits Syst. I 64 (2017) 310-321.
[60] C. Sapsanis, U. Buttner, H. Omran, Y. Belmabkhout, O. Shekhah, M. Eddaoudi, K. N. Salama, A Nafion Coated Capacitive Humidity Sensor on a Flexible PET Substrate 2016 IEEE 59th International Midwest Symposium on Circuits and Systems (MWSCAS), Abu Dhabi, United Arab Emirates (2016) 1-4.

[61] Q.M. Wang, D.M. Shen, M. Bülow, M.L. Lau, S.G. Deng, F.R. Fitch, N.O. Lemcoff, J. Semanscin, Metallo-organic molecular sieve for gas separation and purification, Micropor. Mesopor. Mater. 55 (2002) 217–230.
[62] L. Ge, L. Wang, V. Rudolph, Z. Zhu, Hierarchically structured metal–organic framework/vertically-aligned carbon nanotubes hybrids for CO_2 capture, RSC Adv. 3 (2013) 25360–25366.
[63] R.A. DiLeo, B.J. Landi, R.P. Raffaelle, Purity assessment of multiwalled carbon nanotubes by Raman spectroscopy, J. Appl. Phys. 101 (2007) 064307.
[64] C. Prestipino, L. Regli, J.G. Vitillo, F. Bonino, A. Damin, C. Lamberti, A. Zecchina, P.L. Solari, K.O. Kongshaug, S. Bordiga, Local Structure of Framework Cu(II) in HKUST-1 Metallorganic Framework: Spectroscopic Characterization upon Activation and Interaction with Adsorbates, Chem. Mater. 18 (2006) 1337–1346.
[65] H. Uehara, S. Diring, S. Furukawa, Z. Kalay, M. Tsotsalas, M. Nakahama, K. Hirai, M. Kondo, O. Sakata, S. Kitagawa, Porous Coordination Polymer Hybrid Device with Quartz Oscillator: Effect of Crystal Size on Sorption Kinetics, J. Am. Chem. Soc. 133 (2011), 11932–11935.
[66] J. Nie, X. Meng, R. Zheng, S. Wang, Fast quartz resonant sensors for high humidity range 60–95% RH, Sens. Actuators B 185 (2013) 211–217.

Karumbaiah N. Chappanda is a post-doctoral fellow in Computer, Electrical and Mathematical Sciences and Engineering Division at King Abduallah University of Science and Technology. His research interest include gas sensors, device fabrication and nano-lithography.

Osama Shekhah is a research scientist in Physical Sciences and Engineering Division at King Abdullah University of Science and Technology. His research interest include surface chemistry, material chemistry, thin films, and porous materials.

Omar Yassine is a research scientist in Computer, Electrical and Mathematical Sciences and Engineering Division at King Abduallah University of Science and Technology. His research interest include gas sensors and Microfluidics.

Shashikant P. Patole is a post-doctoral fellow in Computer, Electrical and Mathematical Sciences and Engineering Division at King Abduallah University of Science and Technology. His research interest include synthesis, characterization and applications of SP2 hybridized carbon materials.

Mohamed Eddaoudi is a professor in Physical Sciences and Engineering Division at King Abdullah University of Science and Technology. He also the director of Advanced Membranes and Porous Materials Research Center at at King Abdullah University of Science and Technology.

Khaled Nabil Salama is an Associate Professor and founding chair member in the Electrical engineering department at King Abduallah University of Science and Technology. His research interests include electronic circuit design and semiconductors' fabrication.

Figure captions

Fig. 1. (a) Digital image of the QCM coated with HKUST-1 film. (b) False color SEM micrograph (acquired at 45^{o} tilt) of the QCM coated with HKUST-1 thin film.

Fig. 2. Experimental setup used for characterizing the QCM coated humidity sensor. (a) Schematic of the experimental setup. (b) Digital image of the experimental setup. The components shown in the schematic are number accordingly in the digital image. (c)-(e) Magnified digital images of the test chamber, micro-flow controllers, and humidifier setup, respectively.

Fig. 3. False color SEM micrographs of CNT-HKUST-1 composites. (a) Reduction in the crystal size in regions surrounding the CNT in the very low concentration composite films. (b)-(d) SEM micrographs of CNT-HKUST-1 composite films with 0.5, 1.5, and 2.5 mg of CNT, respectively. The average size of the HKUST-1 crystals is significantly reduced due to presence of uniformly dispersed higher concentration of CNT, increasing the porosity of the films.

Fig. 4. TEM images of CNT-HKUST-1 composite. (a) Cubical HKUST-1 crystals formed on CNT. (b) High resolution image showing the adhesion of the HKUST-1 crystals on to the surface of the CNT.

Fig. 5. Normalized Raman spectra of CNT, HKUST-1 and CNT-HKUST-1 composites. Raman peaks corroborate the integrity of the HKUST-1 crystal formed on the surface of the CNT in the composite films.

Fig. 6. Comparison of the XRD pattern of CNT-HKUST-1 composite thin film with the calculated bulk HKUST-1.

Fig. 7. Comparison of the S_{21} frequency spectrum of CNT, HKUST-1 and CNT-HKUST-1 composites coated QCM sensors at various relative humidity points.

Fig. 8. Comparison of the frequency response based sensitivity of uncoated, CNT, HKUST-1 and CNT-HKUST-1 composites coated QCM humidity sensor.

Fig. 9. Humidity hysteresis curve of QCM sensor coated with 0.5 mg CNT- HKUST-1 thin film.

Fig. 10. Stability of the humidity sensor. (a) Short-term stability of QCM sensor coated with 0.5 mg CNT+ HKUST-1 thin film. (b) Long-term stability of QCM sensor coated with 0.5 mg CNT- HKUST-1 thin film.

Fig. 11. Dynamic behavior of the QCM sensor for characterization of the response and recovery time. The red line shows the response of the commercial humidity sensor for comparison.

Fig. 12. Temperature studies. (a) Effect of temperature on commercial humidity sensor at near zero %RH. (b) The change in sensitivity of the QCM coated with 0.5 mg CNT- HKUST-1 thin film with change in temperature.

Fig. 13. Frequency response of the QCM coated with 0.5 mg CNT-HKUST-1 thin film with change in humidity in air.

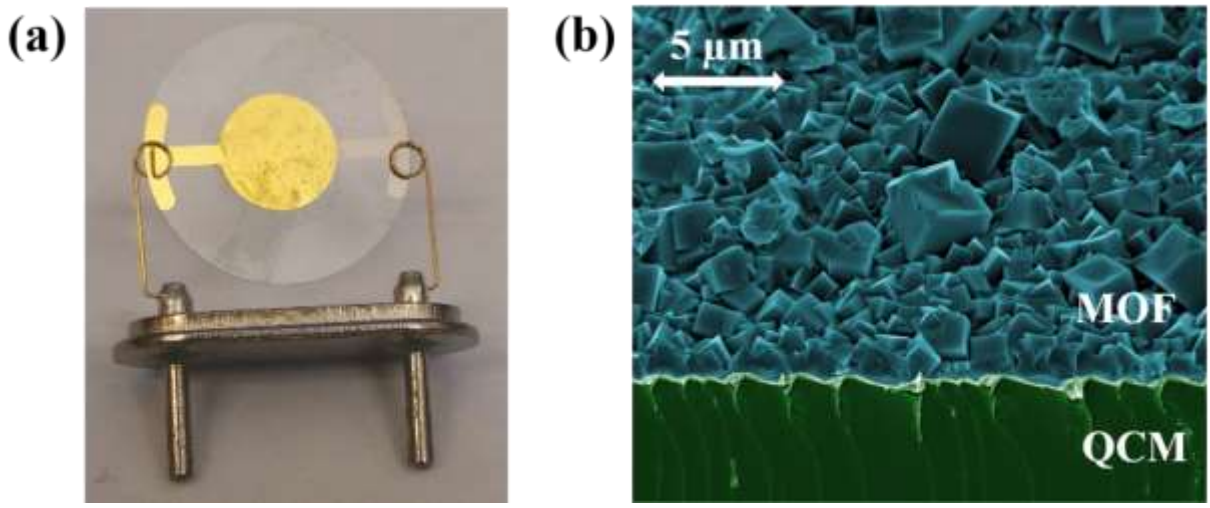

Fig. 1

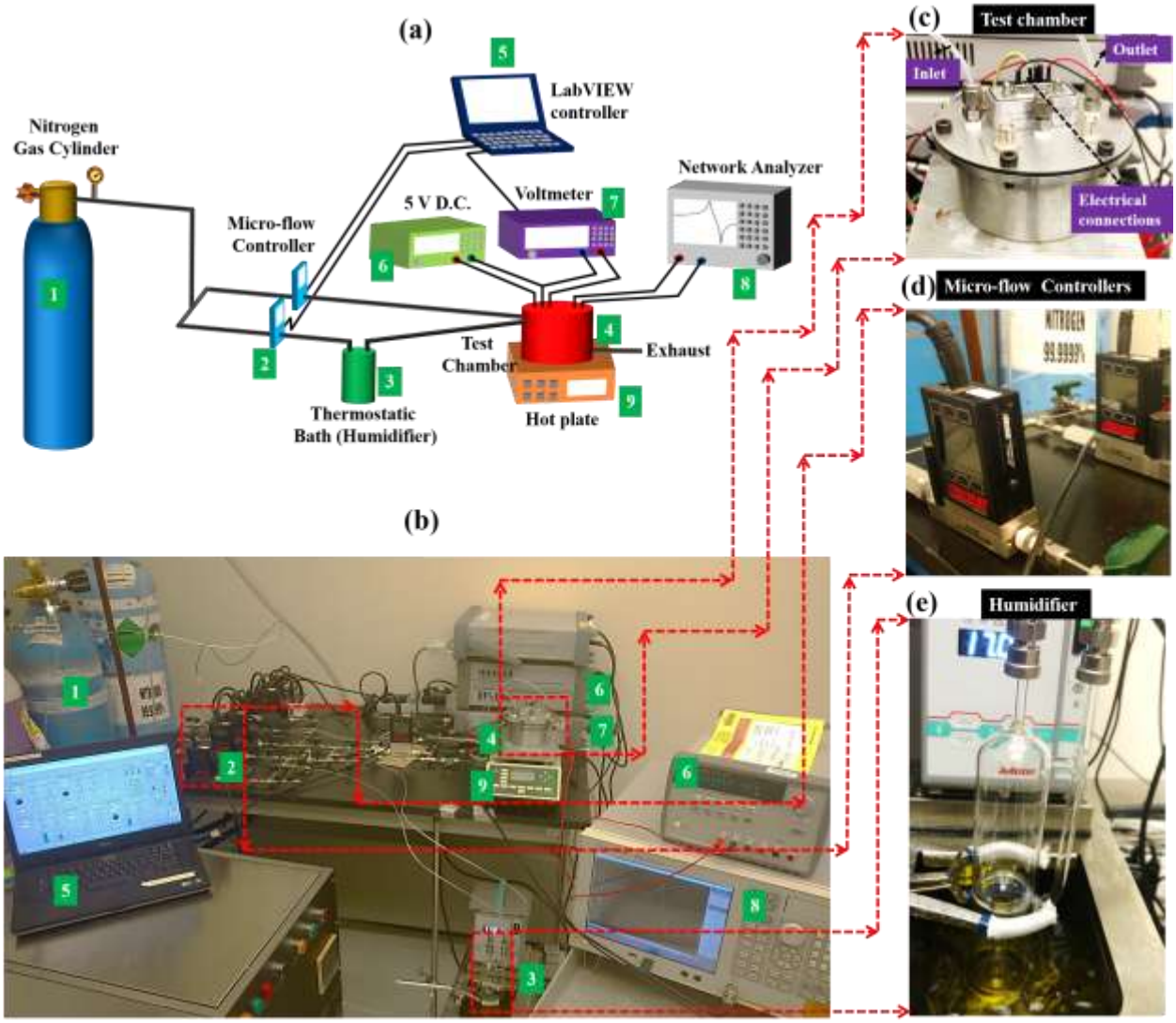

Fig. 2

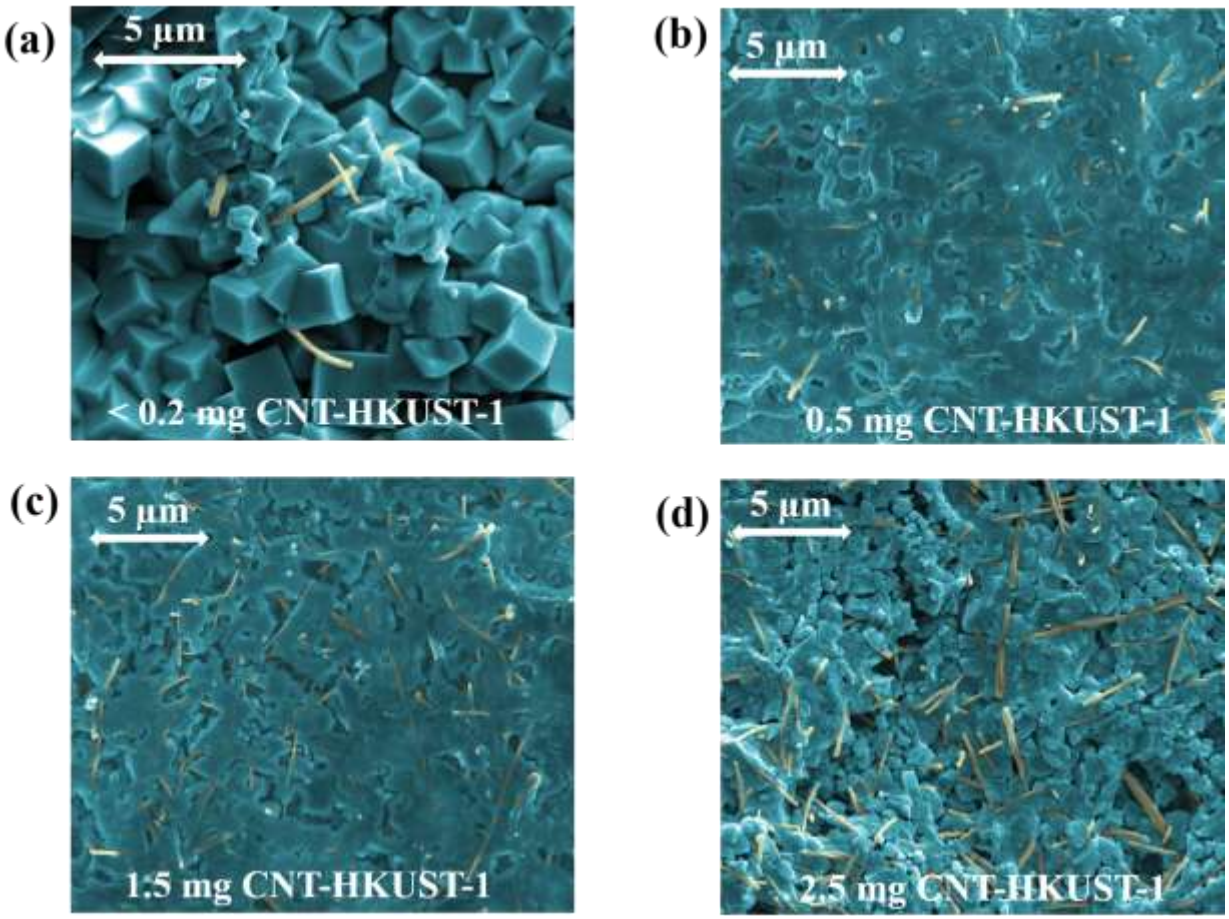

Fig. 3

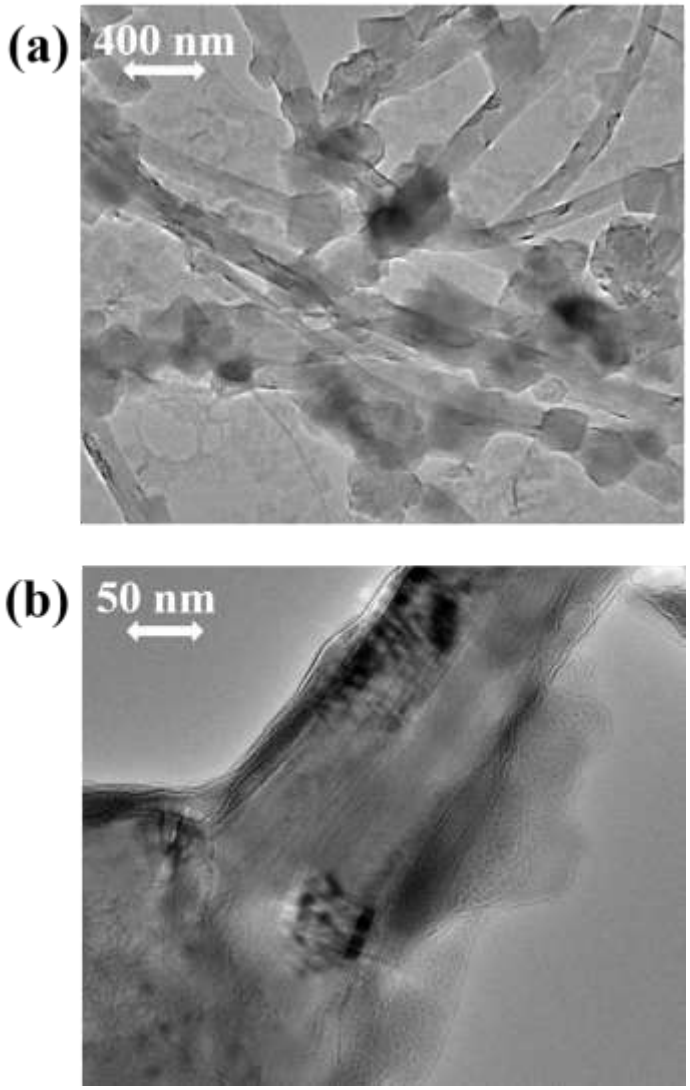

Fig. 4

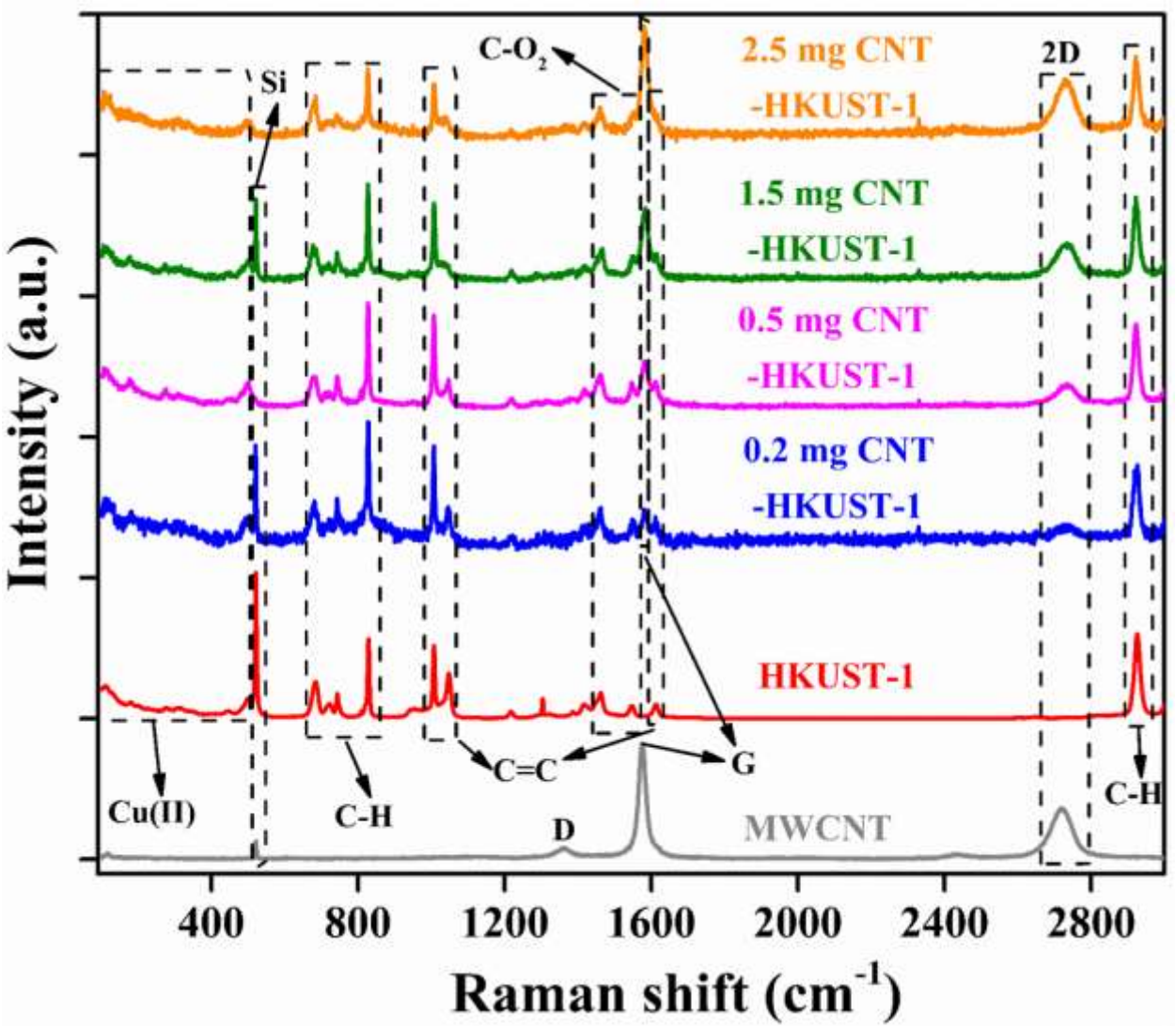

Fig. 5

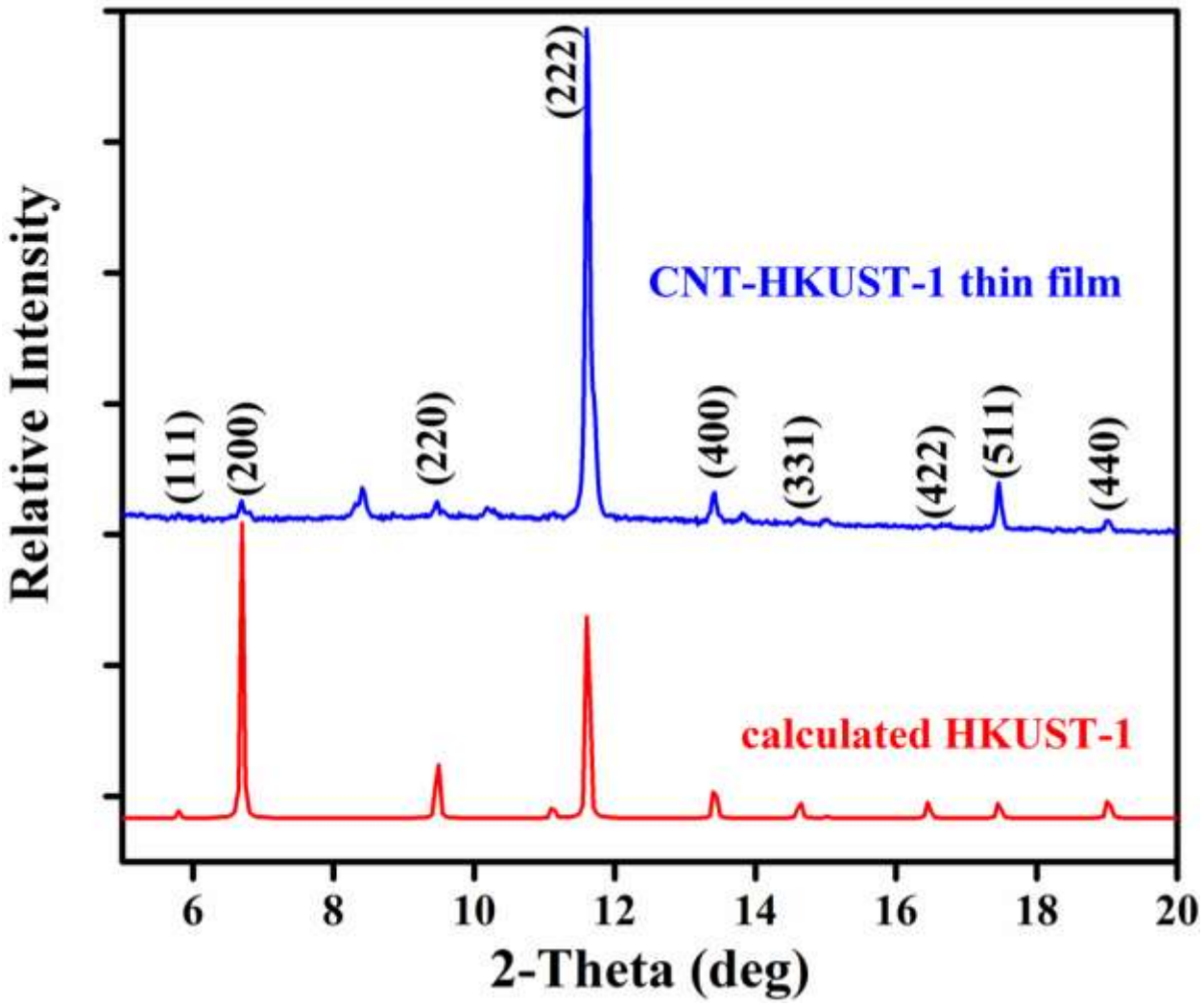

Fig. 6

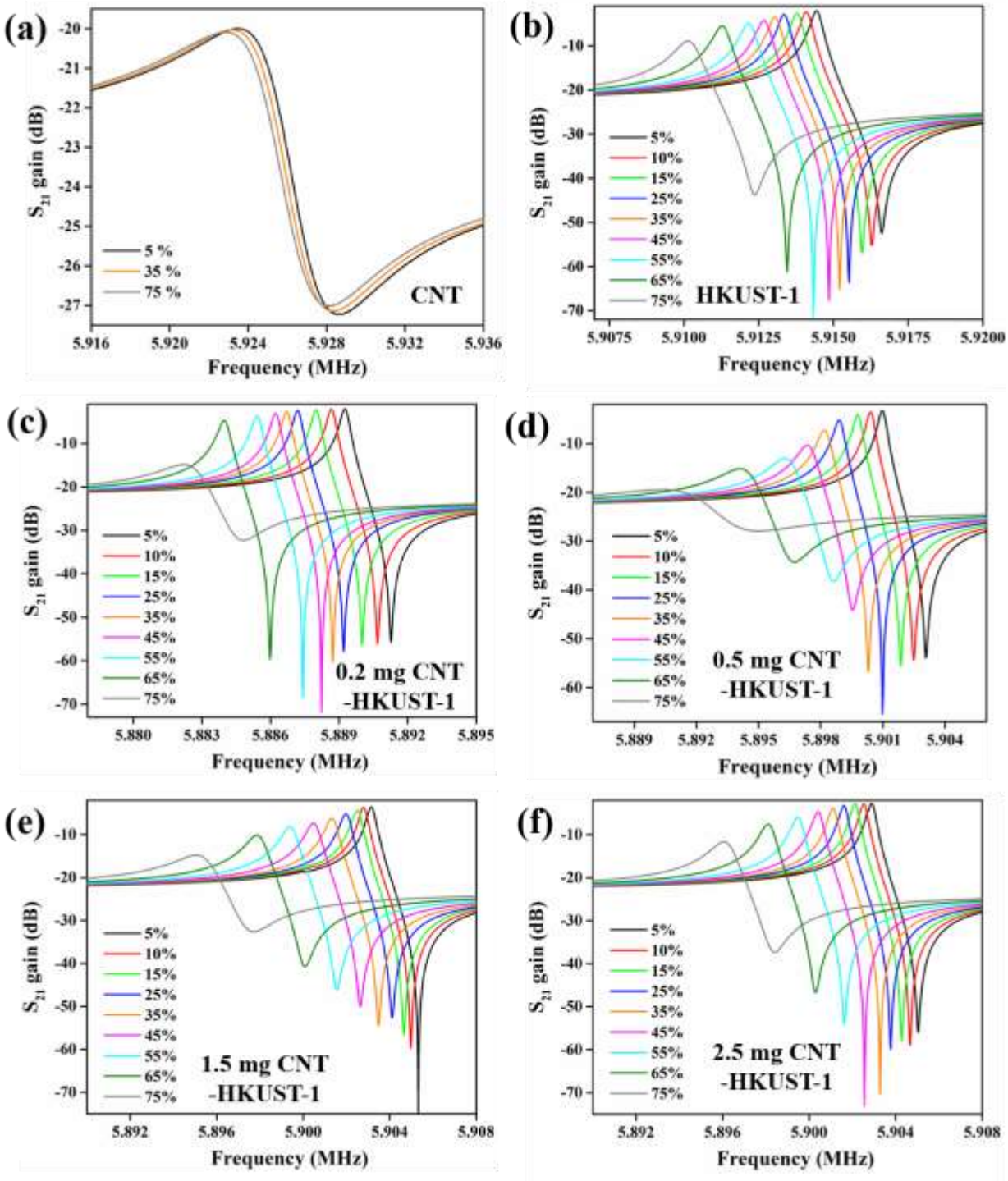

Fig. 7

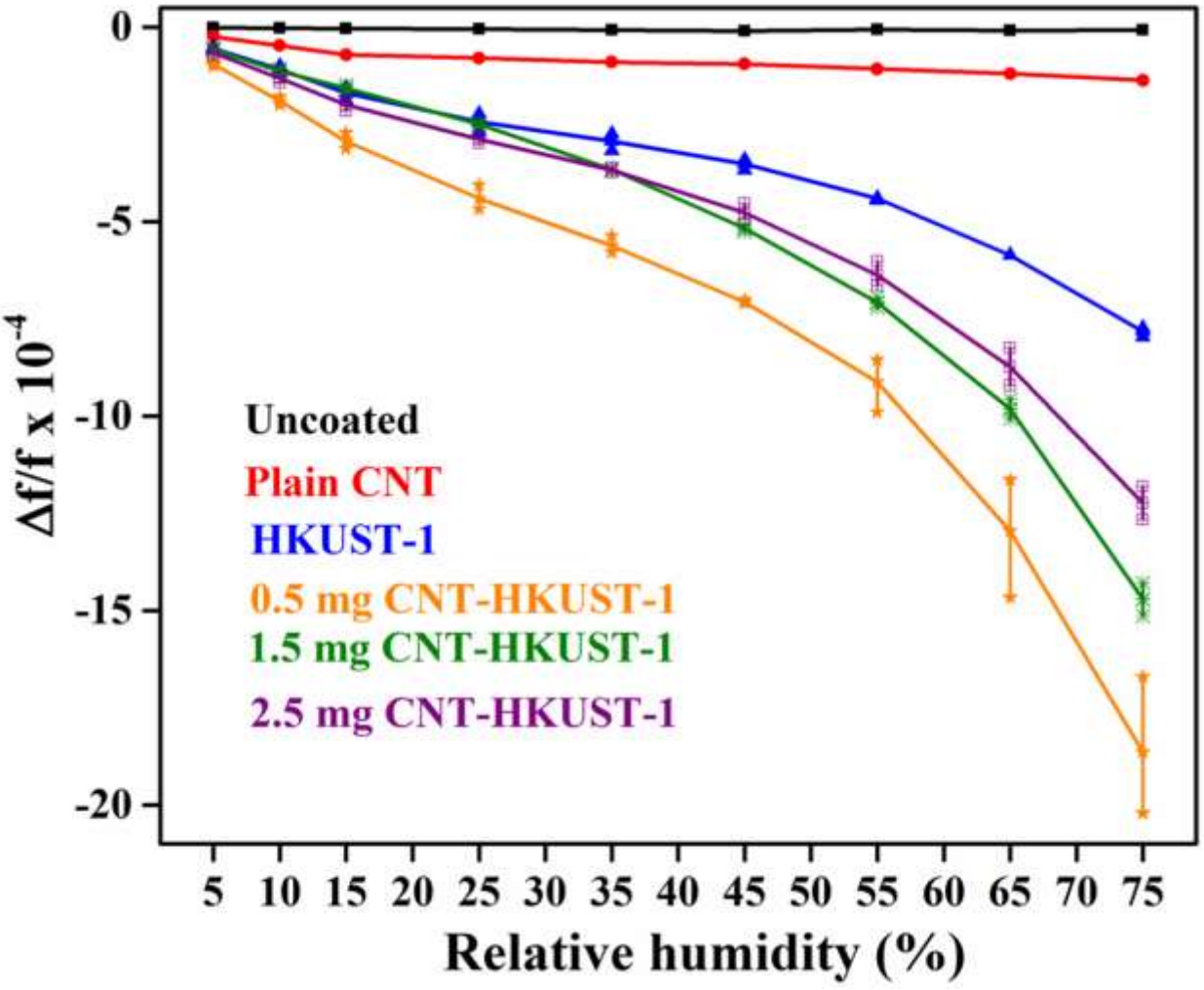

Fig.8

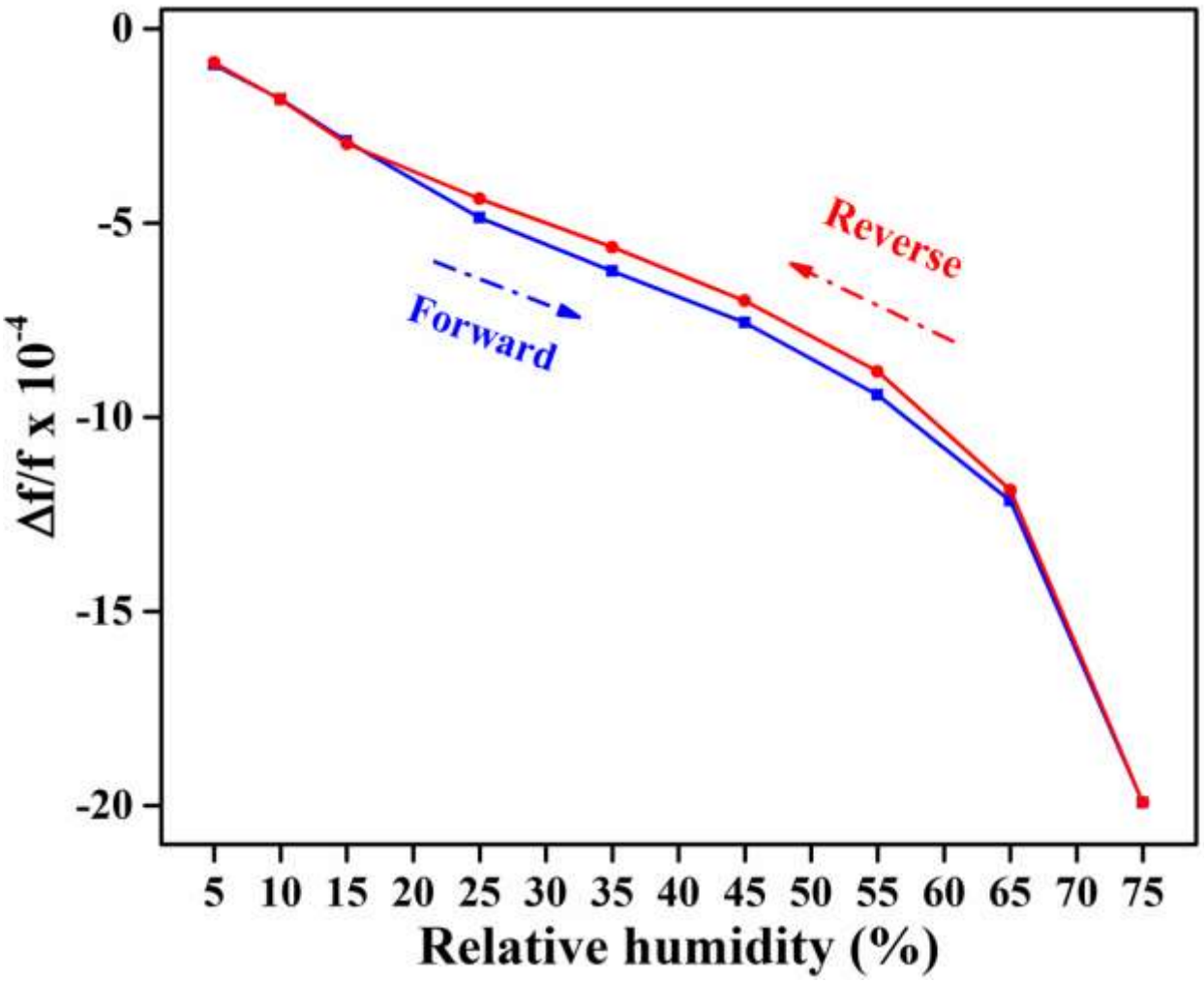

Fig. 9

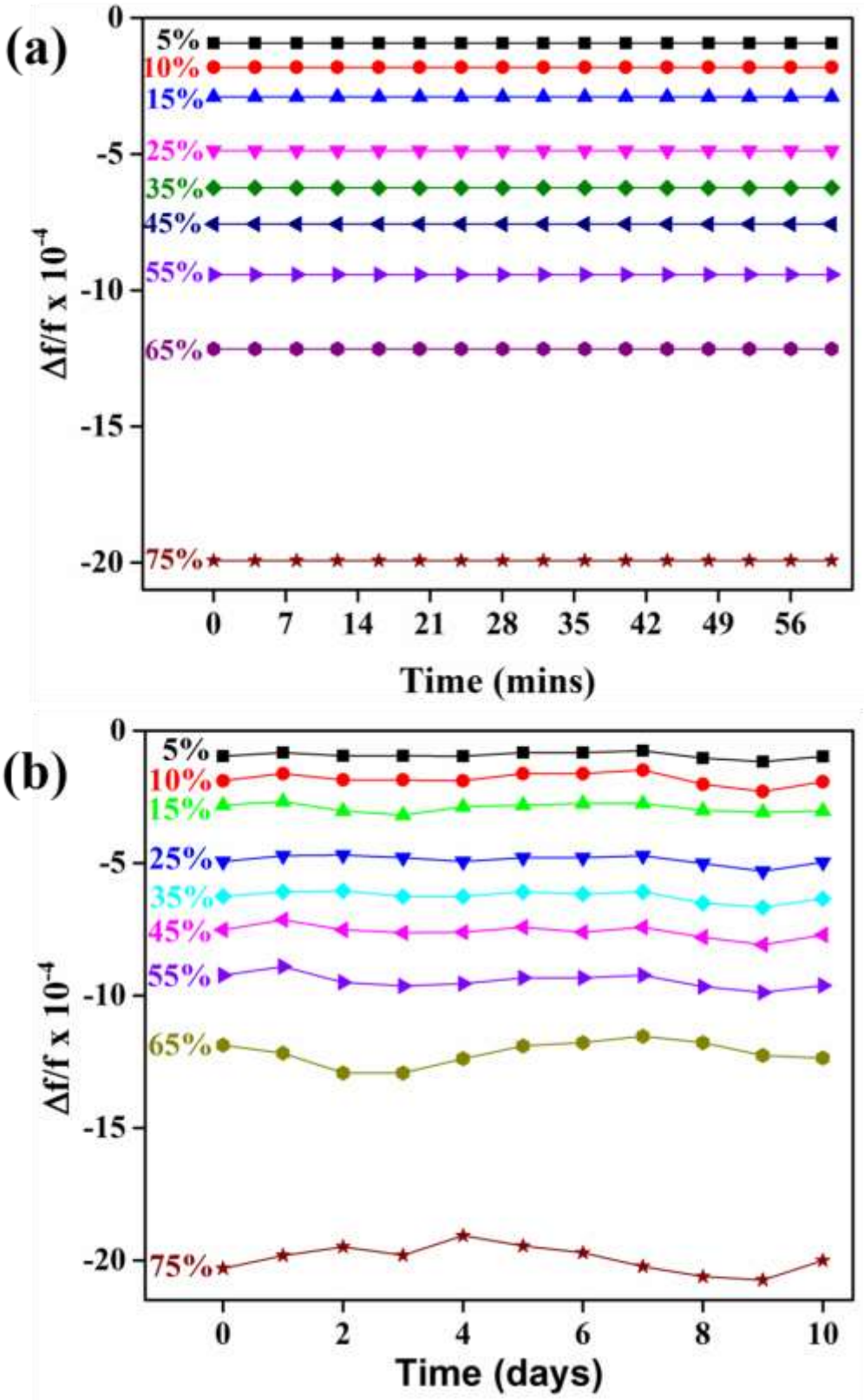

Fig. 10

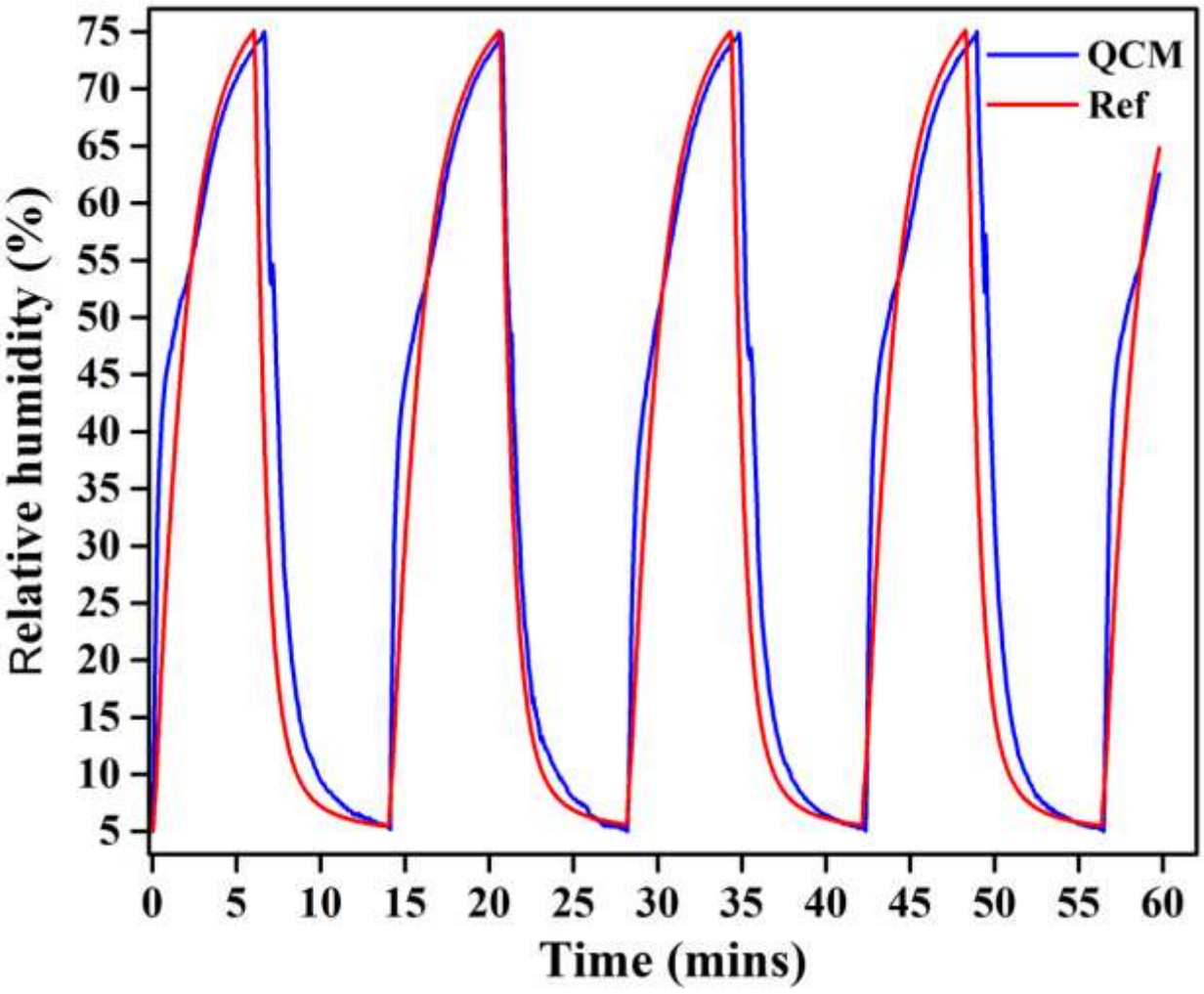

Fig. 11

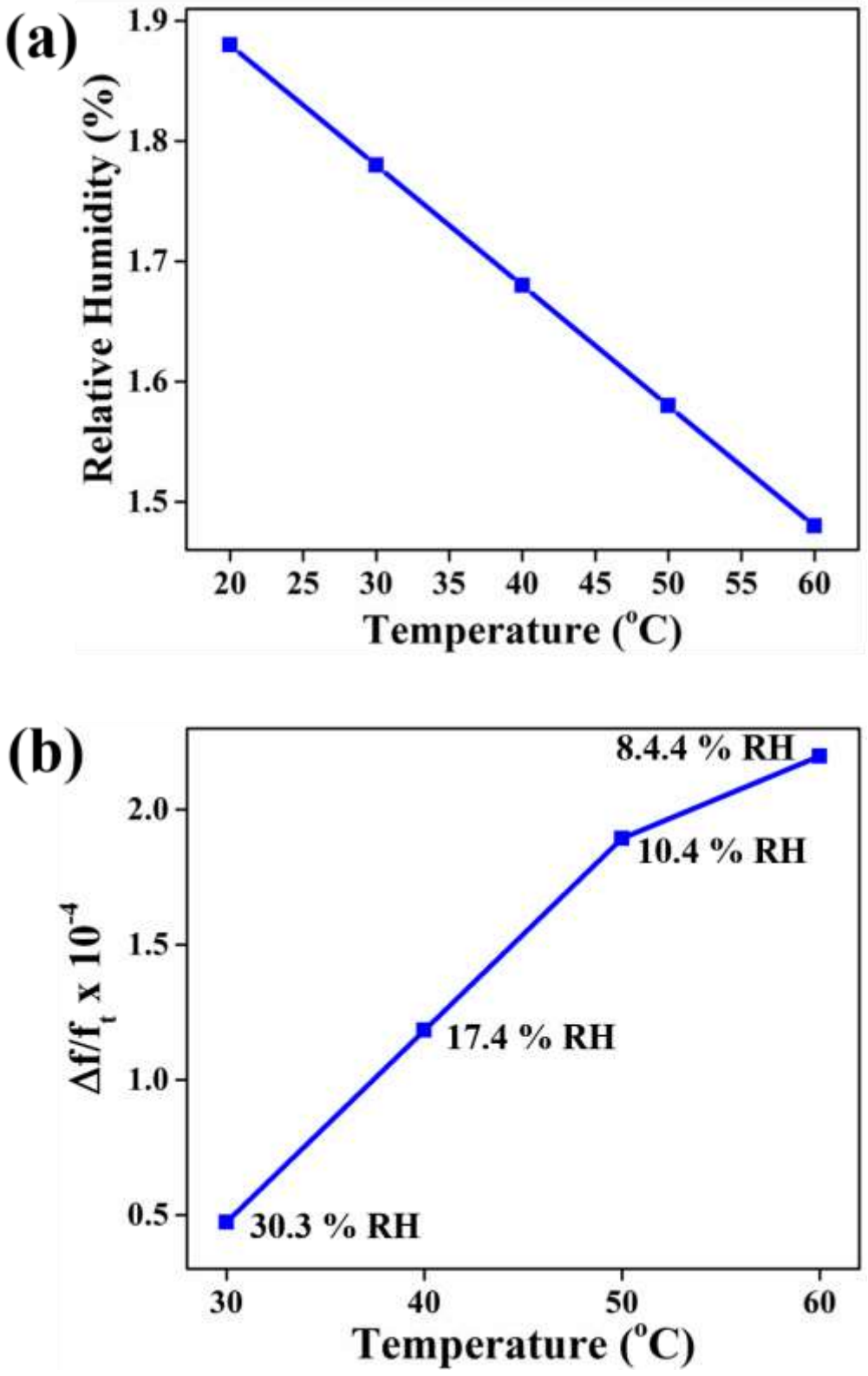

Fig. 12

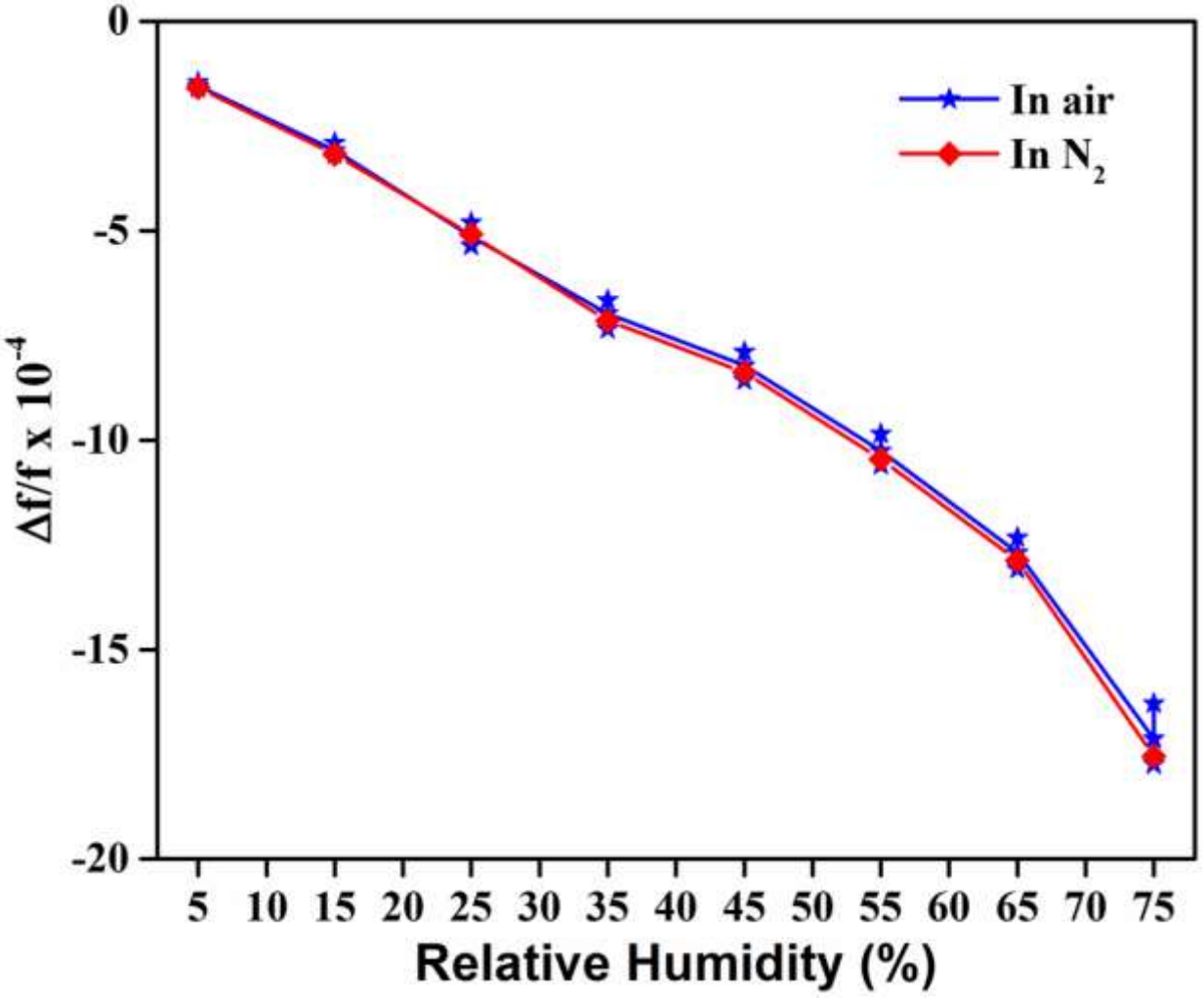

Fig. 13

Table 1. Comparison of the mass of sensing films and adsorbed water wt%.

Humidity sensing film	Sensing film mass (ng)	Mass of adsorbed water at 75% RH (ng)	Adsorbed water wt%
CNT	210	20	10
HKUST-1	420-436	114	27
0.5 mg CNT + HKUST-1	740-783	271	36
1.5 mg CNT + HKUST-1	710-730	214	30
2.5 mg CNT + HKUST-1	697-723	178	25

Table 2. Comparison of the previously reported QCM based humidity sensors.

Ref.	Material coated	RH range (%)	Sensitivity ($\Delta f/f$) per percent RH	Hysteresis (RH %)	Response	Response, recovery time (s)
This work	**MWCNT-HKUST-1 composite**	**5-75**	**25 x 10^{-6}**	**< 5**	**Non-linear**	**250, 265***
[21] Sens. Actuators B 2017	Urea formaldehyde resin/silica composite	11.3-83.6	0.8 x 10^{-6}	< 2	Linear	12, 25
[22] Sens. Actuators B 2017	Phosphorus	11.3-97.3	3.7 x 10^{-6}	< 4	Non-linear	14, 10
[23] Sens. Actuators B 2016	Graphene oxide/poly(ethyleneimine)	11.3-97.3	2.7 x 10^{-6}	< 1	Non-linear	42, 5
[24] J. Sensors 2016	HKUST-1	22-69	8.3 x 10^{-6}	< 30	Non-linear	1676, 1051
[25] IEEE Sensors 2016	Graphene oxide/Nafion composite	11.3-97.3	6.4 x 10^{-6}	< 3	Non-linear	22, 5
[26] Int. J. Electrochem. Sci. 2016	Poly (diphenylamine sulfonic acid), 3- mercaptopropyltrimethoxysilane and nano-Al_2O_3 powder	1-90	53 x 10^{-6}	< 5	Linear	65, 45
[27] IEEE trans. Nanotech. 2014	Nanodiamond films	11.3-97.3	5.1 x 10^{-6}	< 4	Non-linear	25, 3
[28] Mater Sci Semicond Process. 2014	ZnO quantum dots	0-98	5.4 x 10^{-6}	< 6	Non-linear	16, 12
[29] Appl. Phys. A 2012	Poly(diallyldimethylammonium chloride)/SWCNT composite	20.9-80.2	0.25 x 10^{-6}	< 8	Non-linear	NR
[30] J. Mater. Chem. 2011	Polyethyleneimine functionalized polyamide	2-95	4.6 x 10^{-6}	< 4	Non-linear	120, 50
[31] Sens. Actuators B 2011	Bacterial cellulose	5-97	4.4 x 10^{-6}	NR	Non-linear	141, 62
[32] Appl. Surf. Sci. 2011	Graphene oxide film	6.4-93.5	3.1 x 10^{-6}	< 5	Non-linear	18, 12
[33] Nanotechnology 2010	Nanofibrous polyelectrolyte membranes	6-95	3.7 x 10^{-6}	NR	Non-linear	NR
[34] Sens. Actuators B 2010	Mesoporous silica-hexagonal lamelliform	11.3-97.6	6.4 x 10^{-6}	< 4	Non-linear	12, 16
[35] INEC 2008	MWCNT	3-82	5.1 x 10^{-6}	NR	Non-linear	NR
[36] Sens. Actuators B 2008	Polypyrrole/Ag/TiO_2	1-41	1.75 x 10^{-6}	NR	Non-linear	12, 20

[37] Sens. Actuators A 2007	ZnO film	15-85	2 x 10^{-6}	NR	Non-linear	NR
[38] Sens. Actuators A 2005	Ball milling and hydrogen plasma treated MWCNT	5-97	4.3 x 10^{-6}	NR	Linear	60, 70
[39] Sens. Actuators B 2005	CNT/Nafion	0.035-61	20 x 10^{-6}	NR	Linear	5, 5

Note: NR represents "not reported"; *The response and recovery time reported here higher due to the limitation of the maximum flow rate of micro flow controller (200 cm^3/min) from Alicat Scientific Inc. (MCQ-200SCCM-D).